

Influence of Gamma Radiation on Compatibilized LLDPE/Magnesium Hydroxide/Sepiolite Composites

Ishaq Ahmad, Muhammad Shafiq, Tariq Yasin

Advanced Polymer Laboratory, Department of Metallurgy and Materials Engineering,
Pakistan Institute of Engineering and Applied Sciences, P.O. Nilore, Islamabad, Pakistan
Correspondence to: T. Yasin (E-mail: yasintariq@yahoo.com)

ABSTRACT: The influence of gamma irradiation on the properties of compatibilized linear low-density polyethylene/magnesium hydroxide (MH)/sepiolite composites has been investigated. Vinyl triethoxy silane and maleated polyethylene have been used as compatibilizers. The compatibilizing effect in the composites is confirmed by the Fourier transform infrared spectra, which showed the presence of additional chemical bonds, which are responsible for the enhanced polymer-filler interaction. As a result, the miscibility of the polar additives into the nonpolar polymer matrix is enhanced. The scanning electron micrographs revealed that the additives are well embedded and uniformly dispersed in the polymer matrix without any voids. The known thermal decomposition temperature of MH ($\sim 350^\circ\text{C}$) is also increased in the compatibilized composites. In addition, 150 kGy irradiated composite showed a remarkable improvement of 37°C in the onset degradation temperature of unirradiated composite. Furthermore, the formation of radiation cross-linked structure in the composites also improved the mechanical properties of the composites. © 2012 Wiley Periodicals, Inc. *J. Appl. Polym. Sci.* 000: 000–000, 2012

KEYWORDS: compatibilization; composites; flame retardance; polyolefins

Received 24 February 2012; accepted 2 July 2012; published online

DOI: 10.1002/app.38293

INTRODUCTION

The carbonaceous nature of synthetic polymers need flame retardant additives to enhance their flame retardancy. The halogenated flame retardants improve the flame retardancy at lower additive content but face many environmental and health concerns due to their corrosiveness and toxicity issues. But, the non-halogenated flame retardants are less toxic and are environment friendly, when compared with the halogenated ones.^{1–3} Their mode of action is physical and generally a large amount is required to get the adequate flame retardancy. Moreover, the good dispersion of fillers in polymer matrix is required for the satisfactory performance and application of the composites. The self-aggregation of fillers leads to their poor dispersion and thereby weak interfacial adhesion with the polymer matrix. In polyolefin/magnesium hydroxide (MH) composites, the compatibilizers are used to inhibit the aggregation of MH. In this regard, two strategies are adopted; either to modify the filler or the matrix.^{4–7} Yang et al.⁸ applied the first approach and modified the MH with macromolecular compatibilizers and reported remarkable improvement in the properties of linear low-density polyethylene (LLDPE)/MH composites. The matrix-modification strategy is also used, and several studies showed an improvement in the interfacial interaction/adhesion between the polymer matrix

and the fillers.^{9–13} The maleic anhydride and its grafted polymer matrix are most commonly used to enhance the compatibility between MH and polymer matrix in nonhalogenated polyethylene composites.^{14–17} Researcher have also used silane coupling agents to improve the compatibility of polyolefin/MH composites and reported improvement in the dispersion of fillers in the matrix and their adhesion with the polymer matrix.^{18–20}

Our previous work showed the flame retardant synergism between MH and sepiolite in LLDPE matrix.² But, the gamma irradiated composites revealed changes in the MH structure, which also affected the flame retardant efficiency.²¹ In this research, the influence of gamma irradiation on compatibilized LLDPE/Mg(OH)₂/sepiolite composites is studied. Different amount MA-g-PE along with vinyl triethoxy silane (VTES) is added as compatibilizing agents. The effects of compatibilizing agents along with the gamma radiation on the structural, morphological, thermal, and mechanical properties of the composites have been investigated.

EXPERIMENTAL

Materials

LLDPE (LL6201; density = 0.926 g cm^{-3} ; melt flow index = 50 g/10 min) is purchased from Exxon Mobil Chemical (Riyadh, Saudi Arabia). MA-g-PE, VTES, MH, and sepiolite are obtained

from Sigma-Aldrich Chemie (Steinheim, Germany). Irganox-1010 (AO₁) and Irgafos-168 (AO₂) are purchased from Ciba Specialty Chemical (Basel, Switzerland).

Preparation of Composites

The composites are prepared by heat mixing in Thermo Haake Poly-lab Rheomix-600, Internal Mixer (Karlsruhe, Germany) using roller rotors at a constant speed of 60 rpm. First, LLDPE is mixed with 5 or 10 wt % MA-g-PE at 130°C for 3 min. Later, MH (55 phr) parts per hundred parts of polymer, sepiolite (5 phr), stearic acid (1 phr), VTES (1 phr), AO₁ (0.2 phr), and AO₂ (0.1 phr) are added, and the temperature is raised to 170°C for total 20 min. After mixing, the heat pressed sheets are obtained at 170°C under pressure of 200 bar. PE₅ and PE₁₀ identification codes are used to represent the composites containing 5 and 10 wt % MA-g-PE, respectively, and the second digit represent dose absorbed by the composites. The LLDPE formulations is also mixed and pressed under same conditions.

Gamma Irradiation

The irradiation is performed using ⁶⁰Co gamma irradiator (Model JS-7900, IR-148, ATCOP). The composites are irradiated in air at various doses ranging from 25 to 150 kGy at a dose rate of 1.02 kGy h⁻¹.

Fourier Transform Infrared Spectroscopy

The structural analysis is performed using a Nicolet 6700 Fourier transform infrared (FTIR) spectrometer (Thermo Scientific, Waltham, Massachusetts). The FTIR spectra are obtained using attenuated total reflectance mode in the range of 4000 to 400 cm⁻¹ at a resolution of 6 cm⁻¹. Average of 116 scans is reported.

X-Ray Diffraction

The X-ray diffraction patterns of unirradiated and irradiated composites are recorded using X-ray diffractometer (Model: X TRA48, Thermo ARL) with Cu K_α radiation ($k = 1.5406 \text{ \AA}$) operating at 45 kV and 40 mA. The scanning is performed from 5° to 60° at a scanning rate of 1° min⁻¹. The crystallite size perpendicular to the PE and MH planes is calculated using Scherrer's equation, $B(2\theta) = K\lambda/L \cos \theta$, where B is full width at half maxima of peak in radians, θ is angle in degree, and L is crystallite size in nanometer, respectively. The value of K is taken as 0.9.

Morphological Analysis

The morphology of composites is examined using a scanning electron microscope (SEM), JSM 6490LA (JEOL, Japan) at 20 kV. The cryo-fractured samples are coated with gold before analysis. Energy dispersive spectroscopy (EDX) is also performed to investigate the elemental composition at selected point.

Thermogravimetric Analysis

The thermal stability of samples is investigated using thermogravimetric analyzer (Mettler-Toledo TGA/SDTA851^c, Schwarzenbach, Switzerland). The analysis is performed under nitrogen (40 mL min⁻¹) at heating rate of 20°C min⁻¹ from 50°C to 600°C.

Mechanical and Heat Resistance Properties

The mechanical properties are measured at room temperature using a universal tensile testing machine, SANS BSS-500 kg

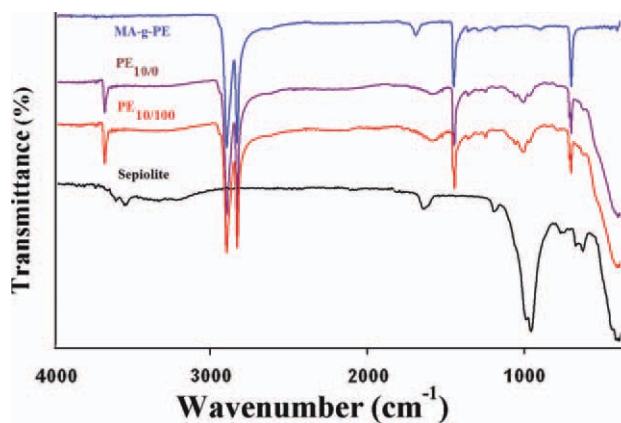


Figure 1. FTIR spectra of MA-g-PE, sepiolite, PE_{10/0}, and PE_{5/100} composites in the range of 4000–500 cm⁻¹ at a resolution of 6 cm⁻¹. [Color figure can be viewed in the online issue, which is available at wileyonlinelibrary.com.]

(SANS Group, China) according to ASTM D-638 at a crosshead speed of 50 mm min⁻¹ using 10 kN load cell. Five specimens are tested for each formulation, and the average results are reported.

The heat resistance testing of the unirradiated and irradiated composites is performed by measuring heat deflection temperature (HDT) and Vicat softening temperature (VST). The HDT and VST values of the composites are measured under a load of 1.8 MPa and 1 kg, respectively. The dimensions of the specimens are according to ISO-306 (80 × 10 × 4 mm), and the temperature of the oil bath is raised at 50°C h⁻¹.

Gel Content Determination

The gel content of irradiated composites is calculated according to ASTM 2765 using Soxhlet apparatus. The samples are extracted in boiling xylene for 8 h, and the gel content is calculated using following formula:

$$\text{Gel content (\%)} = (W_1/W_0) \times 100$$

where W_0 and W_1 are weight of sample before and after extraction, respectively.

RESULTS AND DISCUSSION

FTIR Spectroscopy

The structural analysis is performed using FTIR spectroscopy. The FTIR spectra of maleated polyethylene, sepiolite, unirradiated, and irradiated composites are shown in Figure 1. Maleated polyethylene showed characteristic bands at 2913, 2846, and 1462 cm⁻¹, which are attributed to the C–H stretching and bending vibrations, respectively.²² The band appeared at 1715 cm⁻¹ corresponds to the carbonyl stretching of MA-g-PE.²³ The spectrum of sepiolite showed the O–H characteristic bands attributed to the various types of water in the region of 3700–3300 cm⁻¹ and 800–650 cm⁻¹. The stretching vibrations of Si–O appeared at 1210, 1008, and 976 cm⁻¹ and its bending vibration at 460 cm⁻¹, respectively.²⁴ The unirradiated composite (PE_{10/0}) exhibited all the aforementioned C–H stretching and bending vibrations. A sharp band attributed to the O–H stretching of MH is observed at 3690 cm⁻¹, whereas the other

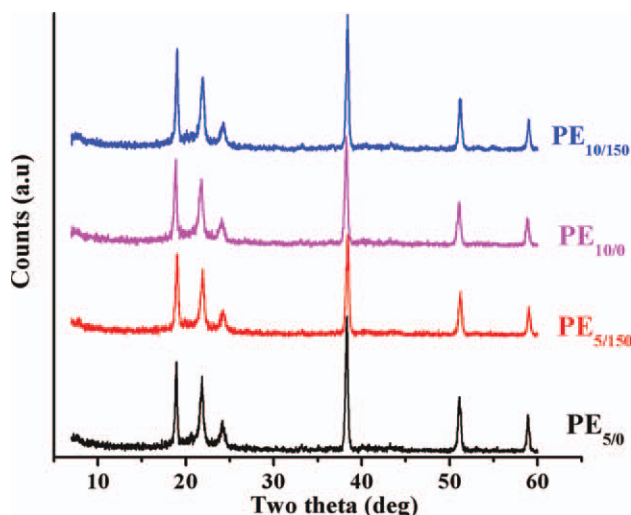


Figure 2. X-ray diffraction patterns of unirradiated and irradiated PE_{5/0}, PE_{5/150}, PE_{10/0}, and PE_{10/150} composites. [Color figure can be viewed in the online issue, which is available at wileyonlinelibrary.com.]

bands in this region (3700–3300 cm⁻¹) are disappeared. Moreover, the composites also exhibited bands at 1020 and 1080 cm⁻¹, which are attributed to the presence of siloxane-linkage.^{2,24,25} It is noteworthy that the band at 1715 cm⁻¹ is disappeared, and a broad band in the range of 1660–1570 cm⁻¹ is observed in the composites, which might be due to the conversion of maleic anhydride group into other acid derivatives and/or carbonyl groups. The formation of these groups in the polymer system changes the polarity and enhanced the polymer-filler interactions. The spectra of irradiated composites (PE_{10/100}) exhibit all the aforementioned bands. But, the intensity of band at 3690 cm⁻¹ is increased in irradiated composites, which might be due to the increase in the number of —OH group that may be generated from sepiolite during irradiation.

X-Ray Diffraction

The X-ray diffraction patterns and the crystallite size estimated from the full width at half maxima of peaks of unirradiated and irradiated composites are presented in Figure 2 and Table I, respectively. The composites exhibited diffraction peaks at 21.8° and 24.0°, which are attributed to the (110) and (200) crystallographic planes of polyethylene, respectively.²⁶ The diffraction peaks appeared at 19.0°, 38.3°, 51.2°, and 59.0° correspond to (001), (101), (102), and (110) crystallographic planes of MH, respectively.^{27,28} The addition of compatibilizers and radiation dose did not change the diffraction peak position suggesting the presence of the same crystal structure of polyethylene and MH in the composites. Moreover, no new peak is emerged in the composites with increase in the amount of compatibilizers and radiation dose. However, the compatibilizers and gamma radiation influenced the crystallite size in the composites. It can be seen from the table that the crystallite size of composites is decreased with increase in the amount of compatibilizer. For example, the value of *L*₁₁₀ and *L*₁₀₁ in PE_{10/100} is 14.46 and 19.56 nm, respectively, compared with the 37.99 and 28.03 in PE_{5/100} composite. This reduction in the crystallite size of composites might be attributed to the good miscibility of added

components.^{29,30} In addition, the variation in the crystallite size of composites is inconsistent with radiation dose.

Morphological Analysis

Figure 3 depicts the SEM micrographs of unirradiated and irradiated PE₁₀ composites. These micrographs show the presence of MH in the form of hexagonal particles and sepiolite in the form of fibers. The additives are well embedded and uniformly dispersed in the polymer matrix without any voids. In addition, the micrographs exhibited the ductile fracture of composites. These findings revealed the good interfacial adhesion between the polymer matrix and additives, which are attributed to the compatibilizers. The radiation-induced morphological changes are also observed in the micrographs of the irradiated composites, wherein the dispersion of fillers is further enhanced. EDX analysis is performed to investigate the elemental composition of the observed hexagonal particles and the fibers in the composites. The EDX of the hexagonal particles showed the presence of magnesium along with silicon (Si) and carbon (C). The presence of C and Si on the hexagonal particle might be from PE and silane [Figure 3(D,E)]. Similarly, the EDX of sepiolite fibers also showed the presence of Mg and C along with the higher concentration of Si [Figure 3(F,G)].

Thermogravimetric Analysis

The thermogravimetric analysis (TGA) and derivative thermogravimetric (DTG) thermograms of neat LLDPE, unirradiated, and irradiated composites are presented in Figure 4, and the thermal stability data obtained from the thermograms is summarized in Table II. This table exhibits the onset degradation temperature (*T*_{onset}), temperature at mass loss of 5%, 10%, and 20% and residue at 550°C. The LLDPE shows mass loss in one step, which is attributed to the decomposition of ethylene backbone and underwent complete degradation with no char residues. The composites exhibited higher (*T*_{onset}), thermal stability and residue compared with the LLDPE. The *T*_{onset} of PE_{10/0} composite is about 10°C higher than that of LLDPE and 24.6% residue was left after the degradation of composite. Moreover, the DTG curves illustrated that the mass loss rate of composites is also lower than that of the LLDPE. This higher thermal stability of composite is due to the presence of inorganic additives. These additives form a glassy layer on the surface of burning

Table I. Crystallite Size and Peak Position Estimated From the X-Ray Diffraction Patterns of the Composites

Sample	Crystallite size (nm)			2θ (°)		
	<i>L</i> ₁₁₀	<i>L</i> ₂₀₀	<i>L</i> ₁₀₁	(110)	(200)	(101)
PE _{5/0}	25.41	16.96	28.99	18.91	21.82	38.30
PE _{10/0}	22.31	14.00	24.30	18.85	21.76	38.30
PE _{5/50}	29.18	16.75	31.14	18.92	21.83	38.30
PE _{10/50}	24.78	13.78	27.12	18.82	21.76	38.20
PE _{5/100}	37.99	14.27	28.03	18.96	21.84	38.32
PE _{10/100}	14.46	11.30	19.56	18.76	21.78	38.42
PE _{5/150}	25.21	24.86	24.74	19.00	21.92	38.37
PE _{10/150}	27.68	15.90	27.13	18.96	21.95	38.37

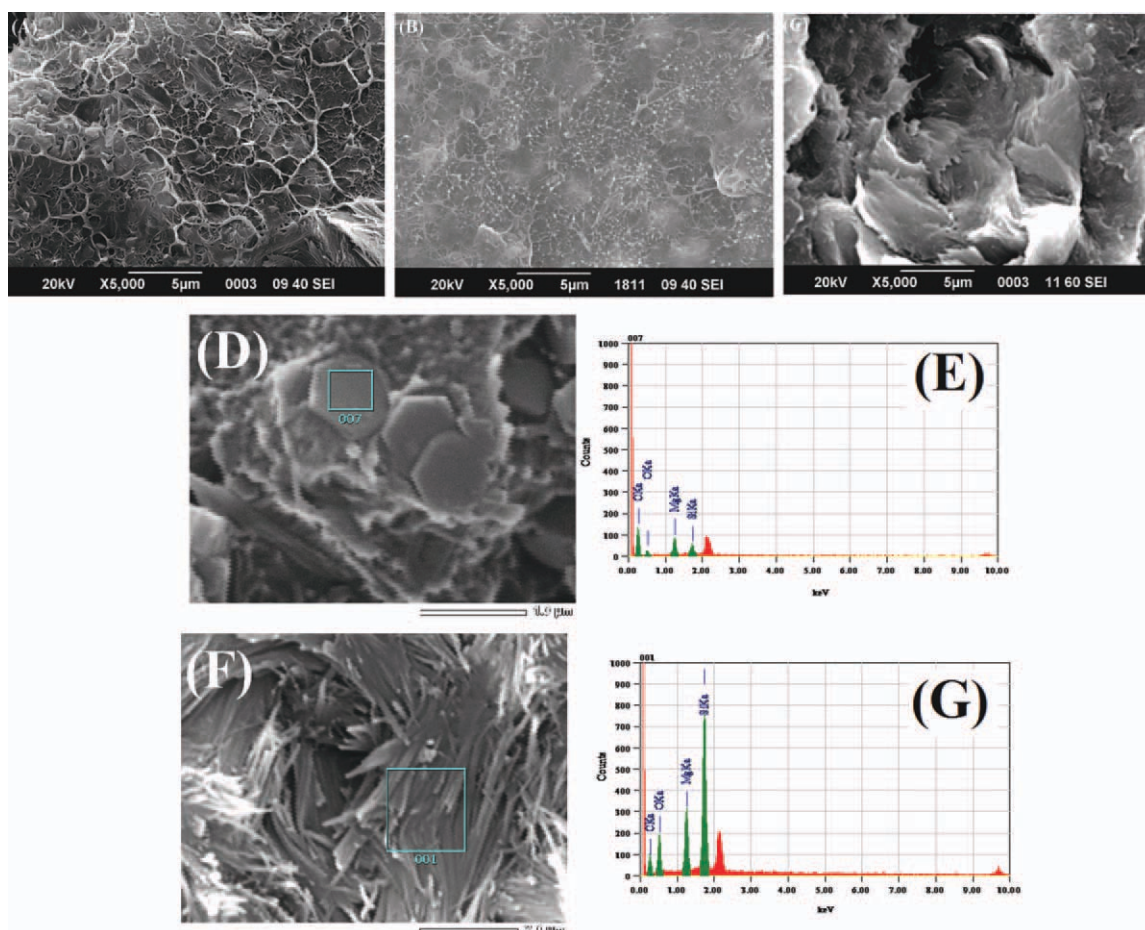


Figure 3. SEMs and EDX spectra of the composites: PE_{10/0} (A), PE_{10/50} (B), PE_{10/150} (C), and EDX spectra PE_{10/0} (E–G). [Color figure can be viewed in the online issue, which is available at wileyonlinelibrary.com.]

polymer matrix, which hold up the release of combustible carbon containing gases and decrease the thermal conductivity of the surface of burning polymer material.^{13,31}

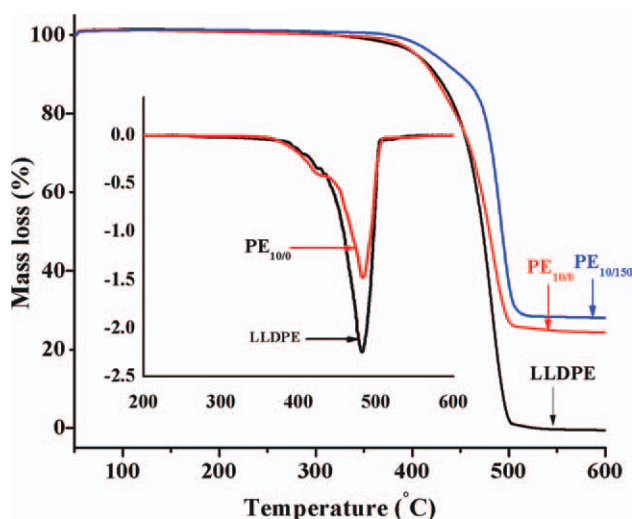


Figure 4. TGA and DTG thermograms of LLDPE, PE_{10/0}, and PE_{10/150} composites. [Color figure can be viewed in the online issue, which is available at wileyonlinelibrary.com.]

The thermogravimetric studies of polyolefin/MH composites showed two-step mass loss, wherein the first step mass loss is generally attributed to the dehydration of MH and the second step mass loss to the polymer backbone chain scission.^{2,21,32} In this study, only one step mass loss is observed in the thermograms, which indicate that the incorporation of compatibilizers have imparted stability to MH, which do not show dehydration before the PE degradation.

In irradiated composites, the T_{onset} and thermal stability are also increased significantly. The T_{onset} of PE_{10/0} is increased

Table II. Thermogravimetric Analysis Results of Unirradiated and Irradiated Composites^a

Sample	T_{onset}	$T_{5\%}$	$T_{10\%}$	$T_{20\%}$	T_{max}	Residue
LLDPE	411.0	404.8	425.0	447.1	481.5	0.0
PE _{10/0}	423.5	404.6	420.7	445.3	479.6	24.6%
PE _{10/50}	457.7	418.1	445.1	473.0	491.0	28.3%
PE _{10/150}	460.2	423.2	450.0	475.4	491.3	28.3%

^aOnset degradation temperature (T_{onset}), temperature at 5% mass loss ($T_{5\%}$), temperature at 10% mass loss ($T_{10\%}$), temperature at 20% mass loss ($T_{20\%}$), temperature at maximum degradation (T_{max}), and residue obtained at 550°C.

Table III. Tensile Strength (TS), Elongation at Break (EB), Heat deflection Temperature (HDT), Vicat Softening Temperature (VST), and Gel Content of the Unirradiated and Irradiated Composites

Sample code	TS (MPa)	EB (%)	HDT (°C)	VST (°C)	Gel content
PE _{5/0}	11.6	4.5	36.0	98.6	–
PE _{5/50}	14.0	5.1	36.3	98.8	43.3
PE _{5/100}	15.3	6.3	37.1	99.0	39.6
PE _{5/150}	15.5	6.8	37.3	99.4	39.2
PE _{10/0}	11.9	6.7	37.1	98.8	–
PE _{10/50}	15.8	6.7	37.5	99.0	43.5
PE _{10/100}	15.9	6.8	37.8	99.1	41.8
PE _{10/150}	16.2	8.3	38.3	99.5	37.1

from 423.5°C to 460.2°C in 150 kGy irradiated composite (PE_{10/150}). Similarly, the T_{20} of PE_{10/0} is increased from 447.1°C to 475.4°C in PE_{10/150} composite. This increase in thermal stability is attributed to the formation of radiation-induced cross-linked network, which further enhanced the barrier effect and delayed the degradation of composites.^{33–35}

Thermomechanical Properties

The mechanical properties such as, tensile strength (TS) and elongation at break (EB) of unirradiated and irradiated composites are presented in Table III. It can be seen from the table that the TS and EB of composites are remained almost constant with increase in the amount of compatibilizer, but it increased with radiation dose. The TS of PE_{10/100} composite irradiated at 100 kGy is increased by 44.5%, when compared with the unirradiated PE_{10/0} composite. This improvement in TS of composites with absorbed dose is attributed to the formation of radiation-induced crosslinked network.

The heat resistance testing of the composites is performed by measuring the heat deflection temperature (HDT) and VST and the values are summarized in Table III. The HDT and VST values of the composites are slightly changed with the incorporation of compatibilizer and gamma irradiation. On the other hand, the HDT and VST values of PE_{10/0} are slightly increased from 37.1°C to 38.3°C and 98.8°C to 99.5°C, respectively, in 150 kGy irradiated composite.

Gel Content

The gel content is generally used to measure the degree of crosslinking in polymer structure. The gel content of irradiated composites is summarized in Table III. This table shows that all irradiated composites exhibited gel content, and the values are in the range of 37% to 46%, which showed the formation of crosslinked network in the composites. The lower gel content value of the composites might be attributed to the presence of large amount of additives, which restricted the crosslinking reactions of macroradicals present on the polymer chain during irradiation.

CONCLUSION

The influence of gamma irradiation and compatibilizers on the structural, morphological, thermal, and mechanical properties of the compatibilized LLDPE/MH/sepiolite composites has been investigated. The compatibilizing effect in the composites is confirmed by the FTIR spectra, which revealed the presence of additional chemical bonds, which are responsible for the enhanced polymer-filler interaction. As a result, the miscibility of the polar additives into the nonpolar polymer matrix is enhanced. X-ray diffraction patterns of composites showed reduction in the crystallite size of the composites with increase in the amount of compatibilizers. The SEM micrographs showed that the additives are well embedded and uniformly dispersed in the polymer matrix without any voids. The TGA results demonstrated an improvement in the thermal decomposition temperature of MH with the addition of compatibilizers. Moreover, an improvement of about 37°C in the T_{onset} of unirradiated composite is seen at 150 kGy absorbed dose. The TS of composites is improved with gamma radiation, whereas it remained constant with increase in the amount of compatibilizer.

REFERENCES

- Puig, C. C.; Albano, C.; Laredo, E.; Quero, E.; Karam, A. *Nucl. Instrum. Meth. B* **2010**, *268*, 1466.
- Gul, R.; Islam, A.; Yasin, T.; Mir, S. *J. Appl. Polym. Sci.* **2011**, *121*, 2772.
- Wang, Z. Z.; Qu, B. J.; Fan, W. C.; Hu, Y.; Shen, X. *Polym. Degrad. Stab.* **2002**, *76*, 123.
- Haworth, B.; Raymond, C. L.; Sutherland, I. *Polym. Eng. Sci.* **2000**, *40*, 1953.
- Berger, S. E.; Petty, H. E. *Organofunctional Silane, Handbook of Fillers for Plastics*, Katz, H. S.; Milewski, J. V. (editors), Van Nostrand Reinhold Company, New York, Chapter 3, 65 (1987).
- Han, G.; Lei, Y.; Wu, Q.; Kojima, Y.; Suzuki, S. *J. Polym. Environ.* **2008**, *16*, 123.
- Hippi, U.; Mattila, J.; Korhonen, M.; Seppala, J. *Polymer* **2003**, *44*, 1193.
- Yang, Z.; Zhou, C.; Cai, J.; Yan, H.; Huang, X.; Yang, H.; Cheng, R. *Ind. Eng. Chem. Res.* **2010**, *49*, 6291.
- Chiang, W. Y.; Hu, C. H. *J. Polym. Res.* **2000**, *7*, 15.
- Mai, K. C.; Qiu, Y. X.; Lin, Z. D. *J. Appl. Polym. Sci.* **2003**, *88*, 2139.
- Fang, Z. P.; Hu, Q. L. *Angew. Makromol. Chem.* **1999**, *265*, 1.
- Shen, H.; Wang, Y. H.; Mai, K. C. *Thermochim. Acta* **2009**, *483*, 36.
- Chen, X.; Yu, J.; Guo, S.; Lu, S.; Luo, Z.; He, M. *J. Mater. Sci.* **2009**, *44*, 1324.
- Lu, H.; Hu, Y.; Xiao, J.; Kong, Q.; Chen, Z.; Fan, W. *Mater. Lett.* **2005**, *59*, 648.
- Li, B.; He, J. *Polym. Degrad. Stab.* **2004**, *83*, 241.

16. Ranadea, A.; Nayakb, K.; Fairbrotherc, D.; D'Souzaa, N. A. *Polymer* **2005**, *46*, 7323.
17. Reddy, M. M.; Gupta, R. K.; Bhattacharya, S. N.; Parthasarathy, R. *Korea Aust. Rheol. J.* **2007**, *19*, 133.
18. Nachtigall, S. M. B.; Miotto, M.; Schneider, E. E.; Mauler, R. S.; Forte, M. M. C. *Eur. Polym. J.* **2006**, *42*, 990.
19. Yang, Z.; Cai, J.; Zhou, C.; Zhou, D.; Chen, B.; Yang, H.; Cheng, R. *J. Appl. Polym. Sci.* **2010**, *118*, 2634.
20. Chen, X. L.; Yu, J.; Guo, S. Y. *J. Appl. Polym. Sci.* **2006**, *102*, 4943.
21. Shafiq, M.; Yasin, T. *Radiat. Phys. Chem.* **2012**, *81*, 52.
22. Alagar, M.; Majeed, S. M. A.; Selvaganapathi, A.; Gnanasundaram, P. *Eur. Polym. J.* **2006**, *42*, 336.
23. Sanchez, Y.; Albano, C.; Karam, A.; Perera, P.; Silva, P.; Gonzalez, J. *Nucl. Instrum. Meth. B* **2005**, *236*, 343.
24. Mir, S.; Yasin, T.; Halley, P. J.; Siddiqi, H. M.; Nicholson, T. *Carbohydr. Polym.* **2011**, *83*, 414.
25. Sirisinha, K.; Chimdist, S. *Polym. Test.* **2006**, *25*, 518.
26. Shafiq, M.; Yasin, T.; Saeed, S. *J. Appl. Polym. Sci.* **2012**, *123*, 1718.
27. An, D.; Wang, L.; Zheng, Y.; Guan, S.; Gao, X.; Tian, Y.; Zhang, H.; Wang, Z.; Liu, Y. *Colloid Surf. A* **2009**, *348*, 9.
28. Ding, Y.; Zhang, G.; Wu, H.; Hai, B.; Wang, L.; Qian, Y. *Chem. Mater.* **2001**, *13*, 435.
29. Saujanya, C.; Imai, Y.; Tateyama, H.; *Polym. Bull.* **2002**, *49*, 69.
30. Xu, W.; Liang, G.; Wang, W.; Tang, S.; He, P.; Pan, W.-P. *J. Appl. Polym. Sci.* **2004**, *88*, 3225.
31. Liu, J.; Zhang, Y. *Polym. Degrad. Stab.* **2011**, *96*, 2215.
32. Liu, H.; Tong, L.; Fang, Z.; Wang, Y.; Noman Alkadasi, N. A. *Polym. Plast. Technol. Eng.* **2008**, *47*, 1097.
33. Coudreuse, A.; Noireaux, P.; Noblat, R.; Basfar, A. *J. Fire Sci.* **2010**, *28*, 497.
34. Lu, H.; Zhang, Q.; Hu, Y. *J. Fire Sci.* **2007**, *25*, 499.
35. Wang, B.; Ti, Q.; Nai, S.; Zhou, K.; Tang, Q.; Hu, Y.; Song, L. *Ind. Eng. Chem. Res.* **2011**, *56*, 5596.